ACS Medicinal Chemistry Letters
Cite This: ACS Med. Chem. Lett. 2019, 10, 481−486
Letter
pubs.acs.org/acsmedchemlett

Improved Selective Class I HDAC and Novel Selective HDAC3 Inhibitors: Beyond Hydroxamic Acids and Benzamides

Alberto Bresciani,[†] Jesus M. Ontoria,[†] Ilaria Biancofiore, Antonella Cellucci, Alina Ciammaichella, Annalise Di Marco, Federica Ferrigno, Alessandra Francone, Savina Malancona, Edith Monteagudo, Emanuela Nizi, Paola Pace, Simona Ponzi, Ilaria Rossetti, Maria Veneziano, Vincenzo Summa, and Steven Harper*

IRBM Science Park, Via Pontina km 30,600, 00071 Pomezia, Rome, Italy

Supporting Information

ABSTRACT: The application of class I HDAC inhibitors as cancer therapies is well established, but more recently their development for nononcological indications has increased. We report here on the generation of improved class I selective human HDAC inhibitors based on an ethylketone zinc binding group (ZBG) in place of the hydroxamic acid that features the majority of HDAC inhibitors. We also describe a novel set of HDAC3 isoform selective inhibitors that show stronger potency and selectivity than the most commonly used HDAC3 selective tool compound RGFP966. These compounds are again based on an alternative ZBG with respect to the *ortho*-anilide that is featured in HDAC3 selective compounds reported to date.

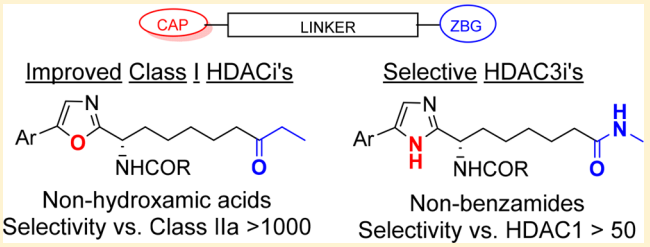

KEYWORDS: *Histone deacetylase, HDAC3 selective, nonhydroxamate, nonbenzamide*

Cellular phenotypes are ultimately controlled by both the cell's genomic DNA sequences and epigenetic factors that have no effect on gene sequence but that do impact gene expression. Epigenetic regulation mechanisms are driven by chemical transformations that structurally modify either DNA itself or the histone proteins around which DNA is packaged in the nucleus of eukaryotic cells.[1] Two enzymes strongly involved in post-translational modification of proteins are histone deacetylases (HDACs) and histone acetyl transferase (HATs). Of the numerous substrates that these enzymes process, their interplay in controlling the acetylation level of lysine residues in the N-terminal tail of histones is of particular importance.[2] Histone acetylation diminishes the charge−charge interactions between nucleic acids in DNA and the positively charged lysine residues in histones and is a key requisite for relaxation of chromatin structure and gene transcription. Favoring histone acetylation, as is expected by inhibition of HDACs, therefore, promotes gene-expression, and HDAC inhibitors continue to nurture extensive interest in drug discovery due to their broad impact on cellular events.

Class I HDACs are predominantly located in the nucleus and are key players in regulating gene expression and cellular differentiation. Class I HDAC inhibitors were originally developed as anticancer agents,[3] and to date four HDACis have been approved for the treatment of cutaneous and peripheral T-cell lymphomas and multiple myeloma.[4] However, the finding that many cancers and most normal cells are relatively resistant to HDACi induced protein hyperacetylation has resulted in a trend toward exploration of HDACis for noncancer indications. While clinical trials initiated prior to 2015 were almost exclusively focused on their use as antiproliferative agents in cancer, ca.70% of post-2015 clinical studies aim to exploit positive pharmacological effects induced by HDACis rather than their (ultimately) cytotoxic properties.[5] At tolerated doses, HDAC inhibitors can still induce gene-expression changes making their use in cases where therapeutic benefit may come from altering a target gene's expression of interest. One example is the use of HDACi for the treatment of Duchenne muscular dystrophy (DMD)[6] where HDAC inhibition is thought to limit the fibro-fatty differentiation of fibro-adipocytic precursors (FAPs) and stimulate the regeneration of muscles by acting on muscle resident satellite cells. Immunological diseases[7] such as encephalomyelitis and rheumatoid arthritis, where HDAC enzymes play a key role in T-cell function, are further examples where inhibitors may prove beneficial.

Despite the therapeutic potential of HDACis, concerns about their use (particularly for class I HDACis) as chronic treatments persist due to known on- and off-target undesired effects. Consequently the development of isoform selective HDAC inhibitors has become the focus of intense recent activity. Subtype-selective HDACis offer the potential for selective pharmacological effects while managing the general mechanism based toxicity associated with HDAC inhibition.[8] Among class I

Special Issue: Highlighting Medicinal Chemistry in Italy

Received: October 31, 2018
Accepted: November 27, 2018
Published: November 27, 2018

DOI: 10.1021/acsmedchemlett.8b00517
ACS Med. Chem. Lett. 2019, 10, 481−486

enzymes the development of HDAC3 selective inhibitors[9] is an attractive goal. It is known that the accessory proteins required to direct HDAC3 activity are different to those used by HDACs 1−2,[10] suggesting that its functions may differ and be associated with specific effects. HDAC3 has been associated with circadian cycle mediated metabolism,[11] inflammation,[12] and CNS diseases.[13] Moreover, in addition to its nuclear function HDAC3 is also found in the cytoplasm[14] suggesting additional roles in post-translationally modifying cytoplasmic targets. HDAC3 activity (though not the entire protein) was shown to be dispensable in HDAC3 inactive mice[15] suggesting that on-target toxicity might be of limited relevance.

We have previously[16] reported on the discovery of what we believe to be the first series of *bona fide* selective *Plasmodium falciparum* HDAC inhibitors (e.g., compound **1**, Figure 1) that

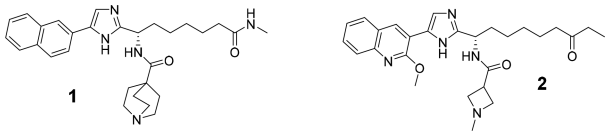

Figure 1. *Pf* HDAC selective and human class I isoform selective HDAC inhibitors.

effectively impeded the growth of malaria parasites in erythrocytes. In tandem with this work (which aimed to avoid human HDAC inhibition), we also focused on developing improved human class I selective and isoform selective inhibitors, predominantly with a view to their use as therapeutic agents for nononcological indications. Here, we describe how SAR from our work toward *Pf* HDAC inhibitors was used in guiding these efforts. We report an evolution of class I HDAC inhibitors (e.g., compound **2**, Figure 1) to provide a new set of potent and highly bioavailable inhibitors of human HDACs 1−3. Our profiling of compound **6**, a preclinical development candidate that demonstrated proof-of-concept in an mdx mouse model for Duchenne muscular dystrophy,[17] is included. In addition, efforts employing information from our *Pf* HDAC (and pan-class I HDACi) work to generate isoform selective inhibitors is described. This led to the discovery of new HDAC3 inhibitors with improved potency and isoform selectivity with respect to benzamide analogs such as RGFP966.[18]

Our past work to generate selective *Pf* HDACis began by screening a structurally divergent subset of our human HDAC inhibitor collection on a *P. falciparum* parasite proliferation assay in erythrocytes. An early hit was compound **3**, an oxazole analog of known[19] alkyl-ketone substituted imidazoles (e.g., **4**) that were themselves designed in our laboratories from apicidin.[20] Replacement of the central imidazole ring in compounds like **4** with alternative five-membered aromatic heterocycles (data not shown) reduced human HDAC1 activity by 5−10-fold for 5-aryl-2-alkyl-1,3,4-oxadiazoles, ca. 10-fold for 5-aryl-2-alkyloxazoles and by 50-fold or more for other heterocycles (triazole, *N*-alkylimidazole, or 1,2,4-oxadiazoles). The oxazole based compound **3** was therefore considered an appealing starting point with a view to favoring *Pf* HDAC vs human HDAC inhibition, and two additional oxazole based analogs (**5**−**6**) were prepared using known SAR from the imidazole series as a guide. Changes to the naphthalene ring (Ar = A in Table 1) and/or to the amide functionality (R in Table 1) were immediately introduced to avoid the high metabolic turnover in liver microsomes that had been a feature of early imidazole compounds.[19]

Table 1. HDAC1 Inhibition and Cellular Class I HDAC Inhibition for Oxazole Based HDACis

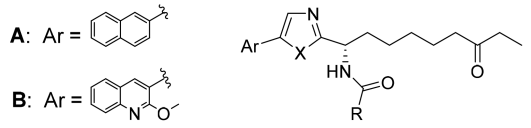

Cpd	Ar	R	X	[a]IC_{50} (nM)	[b]EC_{50} (nM)
[c]2	B	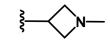	NH	13	135
3	A	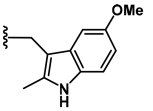	O	19.6	412
4	A	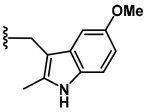	NH	3.2	44
5	A	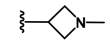	O	12.2	873
6	B	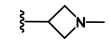	O	1.7	50
7	A	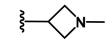	NH	1.5	125
8	B	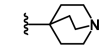	O	1.6	43
9	B	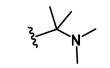	O	3.5	15

[a]HDAC1 IC50 (see Supporting Information for full data with standard deviations). [b]HeLa cellular class I HDAC EC_{50}. [c]See ref 19.

Compounds **5** and **6** ultimately failed to show relevant selectivity in the *P. falciparum* parasite growth assay (with respect to human HDAC assays) and were not further pursued as an avenue toward antiparasitic agents. Intriguingly, however, we observed that 2-methoxyquinoline compound **6** showed stronger than anticipated human HDAC inhibition. While the relative potency of the naphthyl substituted oxazole-imidazole matched pair **5** vs **7** followed the expected trend (around 10-fold weaker potency for the oxazole analog), this was reversed for the 2-methoxyquinoline analogs **6** vs **2**. Testing of further 2-methoxyquinoline substituted oxazole analogs (e.g., compounds **8** and **9**) confirmed that, in the presence of the 2-methoxyquinoline substituent as the aromatic group, the oxazole series was robust in generating strong human class I HDAC inhibition (Table 1). Compounds **6**, **8**, and **9** had IC_{50}s below 3.5 nM against HDAC isoforms 1−3 and were potent inhibitors of class I HDAC's in our HeLa cellular assay. Notably the cellular potency of **9** is almost an order of magnitude stronger than previously reported inhibitors from the related imidazole class (e.g., **2**).

Compound **6** was chosen for further profiling by virtue of its structural analogy with the optimized imidazole **2**. Biochemical studies demonstrated that **6** showed potent inhibition of the class I enzymes HDAC1, 2, and 3 (IC_{50} of 1.7, 2.8, and 1.1 nM, respectively). Strong selectivity against class II HDAC isoforms was measured with **6** having an IC_{50} against HDAC6 of 177 nM

DOI: 10.1021/acsmedchemlett.8b00517
ACS Med. Chem. Lett. 2019, 10, 481−486

and proving inactive at 5 μM against HDACs 4−7. In vitro studies showed that **6** caused no inhibition of metabolic enzymes from the cytochrome P450 (CYP) family with IC_{50}s against CYP isoforms 3A4, 2D6, 2C9, and 1A2, all being >20 μM. Since hydroxamic acid HDACis are typically positive in Ames tests, compound **6** was tested against two strains of bacteria (*Salmonella typhimurium* and *Escherichia coli*). No reverse mutations were detected, highlighting an attractive Ames-negative genotoxicity profile for **6**. Interestingly although the MPO2 score[21] (a recent molecular property based predictor for identifying CNS permeable compounds) for **6** is 4.1 (slightly lower than the preferred value (of 5) for probable brain penetrant compounds), it showed medium-high permeability in a porcine brain endothelial cell blood−brain barrier (BBB) assay ($P = 10.5 \times 10^{-6}$ cm/s).[22] The apparent BBB permeability for **6** suggests that it may provide a path to higher CNS levels than hydroxamic-acid based class I HDACis. The in vivo pharmacokinetic profile for compound **6** is summarized in Table 2. In rat **6** showed 100% bioavailability with a

Table 2. In Vivo[a] PK Parameters for Compound 6

species	F(%)	Clp (mL/min/kg)	Vdss (L/kg)	$t_{1/2}$ (h)	AUC_{po}[b] (μM−h)
mouse	62	13	3.2	3.3	9.3
rat	100	20	5.3	3.3	21.5
minipig	30	20	0.64	3.7	2.6

[a]Compound **6** was dosed as a tartrate salt. [b]Plasma exposure after oral administration of 20, 10, and 5 mg/kg doses in mouse, rat, and minipig, respectively. Data are normalized linearly downward to 5 mg/kg.

3.3 h plasma half-life and moderate (20 mL/min/kg) plasma clearance. In line with its structure, **6** was found to be metabolized by a number of oxidative and dealkylative transformations, but no metabolites were found circulating in rat plasma after sampling 4 h postdose. High oral bioavailability (62%) was also measured in mouse where plasma half-life and clearance were 3.3 h and 13 mL/min/kg, respectively. Modest mouse exposure was a characteristic of previously reported imidazole based compounds, meaning i.p. dosing proved necessary as the administration route for compound **2** in a human HCT116 colon carcinoma mouse xenograft study.[19] The mouse profile for **6** was clearly significantly improved, with a 5 mg/kg oral dose generating an AUC of 9.3 μM·h, 10-fold higher than **2** (AUC 0.9 μM·h). Changing the central scaffold from an imidazole to an oxazole (which replaces a hydrogen bond donor with a hydrogen bond acceptor) improves the PK profile likely by increasing absorption/membrane permeability. Oral bioavailability was retained in larger animals (minipig) where bioavailability was 30% in spite of a potentially significant liver first pass.

An off-target activity for imidazole based compounds such as **2** was *h*ERG potassium ion channel binding (IC_{50} of ca. 3 μM) and in our *h*ERG assay **6** showed a similar IC_{50} of 3.6 μM. In a functional (patch-clamp) assay the IC_{50} for **6** was 10 μM. In contrast, no significant binding (IC_{50} > 16 μM or >30 μM) was measured on a panel of additional ion channels including the sodium $NaV_{1.5}$, calcium $CaV_{1.2}$, and four further K^+ channels. The presence of *h*ERG activity for **6** was not viewed as a hurdle for the advancement of this compound. Based on **6**'s free fraction in human plasma (1.8%), therapeutic doses should result in unbound compound concentrations significantly below the *h*ERG IC_{50}. Nonetheless, the observation of *h*ERG binding for **6** (as well as for a number of further oxazole based analogs on our program) led us to explore approaches to dial out *h*ERG binding from this compound series (Table 3). Chemistry to modulate the

Table 3. Oxazole Based HDACis

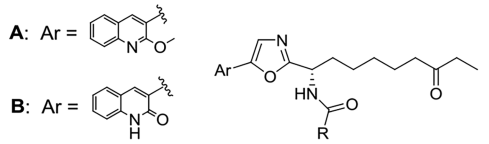

Cpd	Ar	R	IC_{50} (nM)	EC_{50} (nM)	*h*ERG IC_{50} (μM)	[c]pKa	[c]logD
6	**A**		**1.7**	**50**	**3.6**	**7.65**	**3.09**
8	**A**		**1.6**	**43**	**0.19**	**8.81**	**2.78**
10	**B**		**2.1**	**94**	**>30**	**7.64**	**2.63**
11	**A**		**17**	**430**	**13.6**	**4.66**	**3.56**
12	**A**	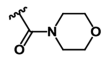	**30.5**	**610**	**>30**	**-**	**2.87**
13	**A**		**3.2**	**208**	**>30**	**-**	**2.65**
14	**A**		**3**	**138**	**>30**	**-**	**3.05**

[a]HDAC1 IC50 (see Supporting Information for full data with standard deviations). [b]HeLa cellular class I HDAC EC_{50}. [c]See ref 23.

moderately basic and lipophilic properties of **6** (calculated[23] pK_a 7.65, calculated logD 3.09) were explored since the combination of these properties are known to be associated with *h*ERG activity.[24] To allow the optimal *N*-methylazetidine amide to be retained, ways to reduce lipophilicity by making structural changes at the oxazole's 2-heteroaryl substituent were explored. Compound **10**, which has the same amine pK_a as **6** but that is less lipophilic (calculated log D 2.63 vs 3.09, respectively), showed that this approach could be successful. Compound **10** had no *h*ERG binding (IC_{50} > 30 μM) but retained cellular class I HDAC potency within 2-fold of **6**. The impact of the basic amine pK_a was clear from strong *h*ERG channel binding (0.19 μM) that was measured for compound **8** (whose amine pK_a is around a log unit higher than **6**, 8.81 vs 7.65, respectively). A marginal improvement in *h*ERG binding came from reducing the pK_a of the azetidine nitrogen in **6** by introducing a fluorine atom on the β-carbon. The lower amine pK_a of **11** vs **6** (4.66 vs 7.65) led to 3−4-fold reduced *h*ERG binding but also impacted HDAC biochemical and cellular potency that were both reduced by an order of magnitude. More success was achieved from SAR to explore compounds containing (alternative) electroneutral amide functionality. A number of compounds of this type did not bind to the *h*ERG channel, with compounds **12**−**14** (all of which have *h*ERG IC_{50}s above 30 μM) providing examples. While compound **12** was somewhat less active against HDACs than compound **6**, the final two compounds in Table 3 showed broadly similar inhibition profiles as **6**, with cellular class I HDAC inhibition within 2−4-fold.

DOI: 10.1021/acsmedchemlett.8b00517
ACS Med. Chem. Lett. 2019, 10, 481−486

Throughout the course of work toward both *Pf* HDACis[16] and human class I HDACis,[19] our compounds were routinely tested on human HDAC isoforms 1−3 (as well as on isoforms from class II HDACs). These data sets were explored in the search for SAR that could lead to the development of isoform selective inhibitors. Figure 2 highlights SAR trends that were the basis for the discovery

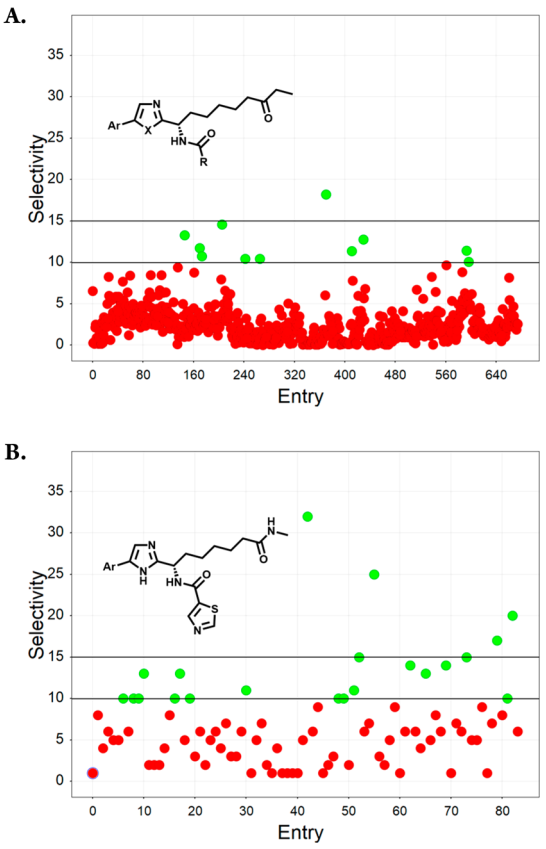

Figure 2. HDAC3 selectivity trends for (A) compounds based on an ethyl ketone ZBGand prepared as human class I HDACis, X = N, O; (B) compounds based on a methyl amide ZBG prepared as *Pf* HDACis.

of HDAC3 selective inhibitors. A consistent profile emerged for compounds that contained an ethyl ketone as their zinc binding group, with essentially equipotent activity being found across HDACs 1−3. Of the 675 ethyl ketone analogs in our collection that were tested on both HDAC1 and HDAC3, only a handful (1.6%) showed 10-fold or higher selectivity (i.e., IC_{50} HDAC1/IC_{50} HDAC3) for HDAC3 (Figure 2A). The lack of robust selective starting points as well as the absence of any clear SAR trends that we could identify (or that stood up to testing) made ethyl ketone analogs a challenging starting point toward selective HDAC3 inhibitors. Similar potencies on HDACs 1−2 were typical for compounds from our work targeting *Pf* HDAC (that were based on an imidazole central core together with a methylamide zinc binding group). However, for these compounds a trend toward stronger inhibition of HDAC3 was evident from a set of 84 analogs that were prepared with a thiazole-5-carboxamide adjacent to the imidazole (Figure 2B). A much larger proportion of this compound set (>20%) was at least 10-fold selective. Higher HDAC3 selectivity than had previously been achieved was observed for a number of compounds, with the 4-*N*,*N*-dimethylmethanaminophenyl compound (**15**, Table 4) proving the best in this set, with 32-fold selectivity. While the amide ZBG appears to favor HDAC3 selectivity, the SAR depicted

Table 4. HDAC3 Selective Inhibitors

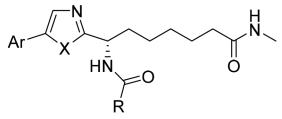

Cpd	Ar	R	X	[a]HDAC1 IC_{50} (nM)	HDAC3 IC_{50} (nM)	[b]Sel
15	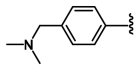		NH	6070	188	32
16	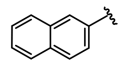		NH	325	235	1.5
17	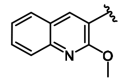		NH	198	24	8
18	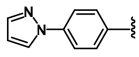		NH	2490	223	11
19	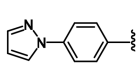	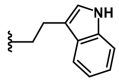	NH	860	42	20
20	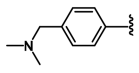	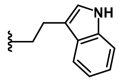	NH	1370	35	39
21	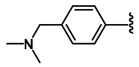	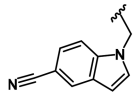	NH	1300	26	50
22	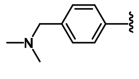	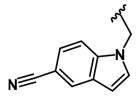	O	13900	3360	4

[a]IC_{50} values are the mean of at least three independent measurements. See Supporting Information for full IC_{50} profiles and standard deviations. [b]Selectivity for HDAC3 (IC_{50} HDAC1/IC_{50} HDAC3).

in Figure 2B illustrates that the nature of the aromatic functionality attached to the central imidazole ring is also important. The evident selectivity measured for **15** was in contrast to the lack of selectivity found for the 2-naphthyl analog **16** (for which the HDAC3 IC_{50} was comparable with HDAC1). Although marginally more selectivity was found for compounds with Ar = 2-methoxy-3-quinoline (e.g., **17**), again these analogs consistently failed to generate highly selective profiles. The origin of selectivity for HDAC3 appears to lie in (stronger) attenuation of HDAC1 activity rather than improved inhibition of HDAC3. Although compounds **15**, **16**, and **18** are similar in terms of their HDAC3 potency, compounds **15** and **18** are less efficient HDAC1 inhibitors. It is perhaps unsurprising therefore that the Ar fragments that feature our most potent HDAC1 inhibitors (such as 2-naphthyl or 2-methoxy-3-quinoline) proved consistently suboptimal with respect to selectivity (see Supporting Information). To explore whether further improved HDAC3 selectivity and improved HDAC3 potency could be achieved, as well as to improve our understanding of SAR, a 2D-array of compounds containing structurally diverse amides (R in Table 4) and either a "highly" selective (cf. compound **15**) or a "moderately" selective (cf. compound **18**) Ar group was prepared. Given the dangers of comparing activity ratios (that are especially sensitive to assay

DOI: 10.1021/acsmedchemlett.8b00517
ACS Med. Chem. Lett. 2019, 10, 481−486

Scheme 1. Synthesis of Oxazole Compounds Containing an Ethyl Ketone ZBG[a]

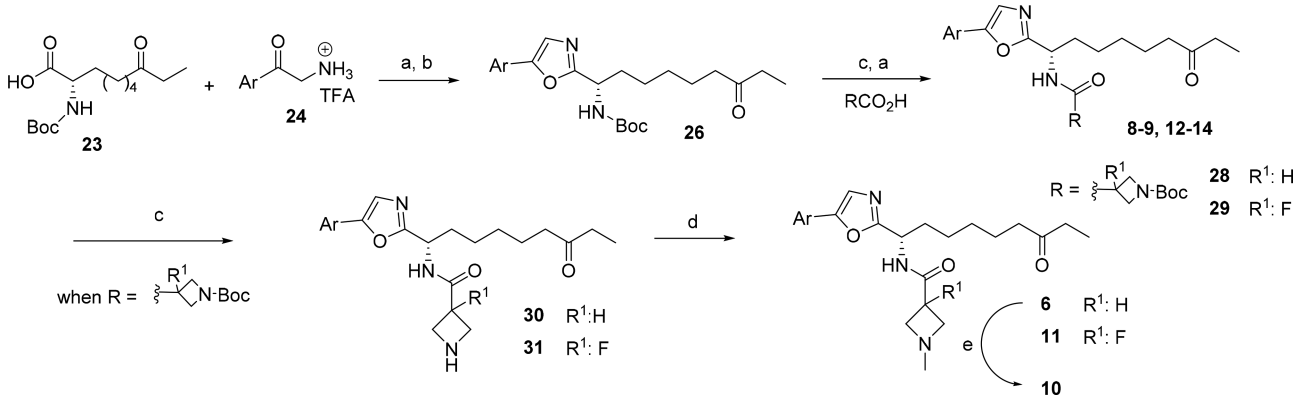

[a]Reagents and conditions: (a) HOBt, EDC, DIPEA, DMF, 20 °C; (b) Ph_3P, C_2Cl_6, TEA, DCM, 20 °C; (c) TFA/DCM (9:1), 0 to 20 °C; (d) HCHO, NaOAc, $NaCNBH_3$, MeOH, 0 to 20 °C; (e) HCl 4 N, DCM, 20 °C.

variability) compounds were in all cases tested in at least triplicate. Compounds **19**−**21** illustrate some of the findings from this set of 60 compounds, more than a third of which generated HDAC3 selectivity above 10-fold. In virtually all cases the 4-*N*,*N*-dimethylmethanaminophenyl analogs generated improved selectivity with respect to the corresponding 4-pyrazolophenyl, though in many cases the improvement was marginal. It is clear from the work we have conducted that achieving HDAC3 selectivity requires the correct zinc-binding group, aryl substituent, and pendant amide. However, the SAR was not without trends that could be followed. While the presence of a basic amine in the aryl fragment was associated with high selectivity for compound **15**, basic groups in the amide R fragment consistently failed to generate selective profiles. Amides R that did generate high selectivity (arbitrarily defined as >15-fold) in the presence of the 4-pyrazolophenyl Ar-group always generated high selectivity in the presence of the 4-*N*,*N*-dimethylmethanaminophenyl Ar-fragment (see Supporting Information). Examples included compounds **19**−**20** that were 20-fold and 39-fold selective, respectively.

Compound **21** provided a further example of a 50-fold selective HDAC3 inhibitor that emerged from this work, and it was encouraging that the improved selectivity for analogs **20** and **21** also aligned with improved potency against HDAC3 with respect to **15** (26 and 28 nM vs 162 nM, respectively). In view of the benefits we have described herein for replacement of the central imidazole core with an oxazole, a final compound that was made was analog **22**. In this case significantly poorer HDAC3 potency and selectivity were found for **22**, suggesting that the imidazole core is preferred for selective profiles.

Compound **21** showed weak inhibition of HDAC2 (IC_{50} of 4.1 μM, 160-fold selectivity over HDAC3) and had IC_{50} > 15 μM against HDAC isoforms 4−7. In line with its weak potency against HDAC1−2 in biochemical assays, low activity was also measured for **21** in our cellular class I HDAC assay (IC_{50} 12 μM). The lower concentration of HDAC3 with respect to isoforms 1 and 2 in the HeLa cells in which the assay is run is expected to desensitize the assay to HDAC3-selective inhibitors. However, at concentrations of **21** that did not inhibit class I HDAC's intracellularly (1 μM), changes in the expression of *UCP1* (a gene whose transcription has been demonstrated to be dependent[25] on HDAC3) were apparent, giving a first indication of HDAC3 selective effects in a cellular context. Compound **21** demonstrated good stability in vitro, proving stable ($t_{1/2}$ > 4 h) in both plasma and hepatocytes from mouse and humans. In view of its strong selectivity and early profile, compound **21** represents a novel lead for the development of HDAC3 selective inhibitors.

The synthesis of oxazole analogs containing the ethyl ketone zinc binding group is outlined in Scheme 1. Amide coupling between Boc-protected L-Aoda amino acid **23** and the appropriate aryl α-aminoketone **24** was followed by ring closure of the β-ketoamide intermediate to furnish the 2,5-disubstituted 1,3-oxazole **26**. Elaboration of the amino substituent by TFA-mediated deprotection followed by amide coupling with the appropriate carboxylic acid gave compounds **8**−**9** and **12**−**14** together with the azetidine precursors **28**−**29**. The azetidine analogs were further elaborated by N-deprotection followed by reductive amination with formaldehyde to give compounds **6** and **11**. Acid-mediated hydrolysis of **6** afforded the 2-quinolinone analog **10**.

Modification of the above route by employing (*S*)-2-((benzyloxy)carbonyl)amino-8-(*tert*-butoxy)-8-oxooctanoic acid in place of **23** was used for the synthesis of oxazole analog **22** (see Supporting Information). The methylamide based compounds **15**−**21** reported in Table 4 were prepared as we have previously described.[16]

In summary, we have reported herein work that led to an advanced set of nonhydroxamic acid class I HDAC inhibitors (exemplified by compound **6**) that show improved pharmacokinetics and cellular activity with respect to previously reported compounds from this class. We found that *h*ERG binding, an undesired off-target biological activity, could be dialed out from this compound series without a strong compromise in terms of HDAC activity profiles. Overall, the profile of the potential clinical candidate **6** compares favorably with current clinical HDAC inhibitors, including Panobinostat.[4] We also reported how a change to the zinc-binding group discovered originally in the context of work toward *Pf* HDAC inhibitors could be employed as a key first step toward biasing SAR for HDAC3 selective profiles. Although SAR in this direction was capricious (with apparently small structural changes having a large impact on activity profiles) following SAR trends allowed us to identify robustly HDAC3 selective compounds for further optimization. Notably, compound **21** was a 26 nM inhibitor of HDAC3 and was 50-fold selective, data that compare favorably with perhaps the most common HDAC3-selective tool compound RGFP966[9,18] (that when tested head-to-head in our assays showed an HDAC3 IC_{50} of 118 nM and was 20-fold selective).

DOI: 10.1021/acsmedchemlett.8b00517
ACS Med. Chem. Lett. 2019, 10, 481−486

■ ASSOCIATED CONTENT

Supporting Information

The Supporting Information is available free of charge on the ACS Publications website at DOI: 10.1021/acsmedchemlett.8b00517.

Synthetic details, biological protocols, IC_{50} data, SAR graphics (PDF)

■ AUTHOR INFORMATION

Corresponding Author

*Phone: +39 06 91093625. E-mail: s.harper@irbm.it.

ORCID

Steven Harper: 0000-0002-1239-0777

Author Contributions

†A.B. and J.M.O. assisted manuscript preparation, data interpretation, and project overview. These authors contributed equally. A.F., HDAC3 selectivity. A.D.M. and A.Ce., in vitro profiling and *h*ERG. E.M. and M.V., DMPK studies. I.B., I.R., A.Ci., S.P., and F.F., Compound synthesis. S.M., E.N., and P.P., compound synthesis, supervision, and target design. V.S., project overview. S.H., manuscript preparation, data interpretation, and project overview. All authors have approved the final version of the manuscript.

Funding

Parts of this work received financial support from the Italian National Compound and Screening Collection (CNCCS consortium) and through the RESEARCH project (Life2020, POR FESR 2014/2020 regione Lazio).

Notes

The authors declare no competing financial interest.

■ ACKNOWLEDGMENTS

We acknowledge Fabrizio Colaceci, Maria Vittoria Orsale, and Roberto Speziale (in vivo work and bioanalysis); Ivan Fini and Odalys Gonzalez (BBB assay); Maria Rosaria Battista (CYP1A2 assay); Nadia Gennari, Ottavia Cecchetti, and Daniela Natale (HDAC assays/HDAC3 biology); Costanza Iaccarino and Letizia Lazzaro (compound purification and QC); and Sergio Altamura, whose science and inspiration were universally appreciated and are missed.

■ ABBREVIATIONS

HDAC, histone deacetylase; *h*ERG, human ether-a-go-go related gene ion channel; *Pf*, *Plasmodium falciparum*; ZBG, zinc binding group

■ REFERENCES

(1) Goldberg, A. D.; Allis, C. D.; Bernstein, E. Epigenetics: a landscape takes shape. *Cell* **2007**, *128*, 635−638.

(2) Allis, C. D.; Jenuwein, T. The molecular hallmarks of epigenetic control. *Nat. Rev. Genet.* **2016**, *17*, 487−500.

(3) Weichert, W. HDAC expression and clinical prognosis in human malignancies. *Cancer Lett.* **2009**, *280*, 168−176.

(4) Tandon, N.; Ramakrishnan, V.; Kumar, S. K. Clinical use and applications of histone deacetylase inhibitors in multiple myeloma. *Clin. Pharmacol.: Adv. Appl.* **2016**, *8*, 35−44.

(5) Abend, A.; Kehat, I. Histone deacetylases as therapeutic targets–from cancer to cardiac disease. *Pharmacol. Ther.* **2015**, *147*, 55−62.

(6) Mozzetta, C.; Consalvi, S.; Saccone, V.; Tierney, M.; Diamantini, A.; Mitchell, K. J.; Marazzi, G.; Borsellino, G.; Battistini, L.; Sassoon, D.; Sacco, A.; Puri, P. L. Fibroadipogenic progenitors mediate the ability of HDAC inhibitors to promote regeneration in dystrophic muscles of young, but not old Mdx mice. *EMBO Mol. Med.* **2013**, *5*, 626−639.

(7) Ellmeier, W.; Seiser, C. Histone deacetylase function in CD4+ T cells. *Nat. Rev. Immunol.* **2018**, *18*, 617−634.

(8) Marx-Blümel, L.; Marx, C.; Kühne, M.; Sonnemann, J. Assessment of HDACi-Induced Cytotoxicity. *Methods Mol. Biol.* **2017**, *1510*, 23−45.

(9) Cao, F.; Zwinderman, M. R. H.; Dekker, F. J. The Process and Strategy for Developing Selective Histone Deacetylase 3 Inhibitors. *Molecules* **2018**, *23*, 551−564.

(10) Watson, P. J.; Fairall, L.; Santos, G. M.; Schwabe, J. W. R. Structure of HDAC3 bound to co-repressor and inositol tetraphosphate. *Nature* **2012**, *481*, 335−340.

(11) Montgomery, R. L.; Potthoff, M. J.; Haberland, M.; Qi, X.; Matsuzaki, S.; Humphries, K. M.; Richardson, J. A.; Bassel-Duby, R.; Olson, E. N. Maintenance of cardiac energy metabolism by histone deacetylase 3 in mice. *J. Clin. Invest.* **2008**, *118*, 3588−3597.

(12) Schuetze, K. B.; McKinsey, T. A.; Long, C. S. Targeting cardiac fibroblasts to treat fibrosis of the heart: focus on HDACs. *J. Mol. Cell. Cardiol.* **2014**, *70*, 100−107.

(13) Malvaez, M.; McQuown, S. C.; Rogge, G. A.; Astarabadi, M.; Jacques, V.; Carreiro, S.; Rusche, J. R.; Wood, M. A. HDAC3-selective inhibitor enhances extinction of cocaine-seeking behavior in a persistent manner. *Proc. Natl. Acad. Sci. U. S. A.* **2013**, *110*, 2647−2652.

(14) Karagianni, P.; Wong, J. HDAC3: taking the SMRT-N-CoRrect road to repression. *Oncogene* **2007**, *26*, 5439−5449.

(15) Sun, Z.; Feng, D.; Fang, B.; Mullican, S. E.; You, S.-H.; Lim, H.-W.; Everett, L. J.; Nabel, C. S.; Li, Y.; Selvakumaran, V.; et al. Deacetylase-independent function of HDAC3 in transcription and metabolism requires nuclear receptor corepressor. *Mol. Cell* **2013**, *52*, 769−782.

(16) Ontoria, J. M.; Paonessa, G.; Ponzi, S.; Ferrigno, F.; Nizi, E.; Biancofiore, I.; Malancona, S.; Graziani, R.; Roberts, D.; Willis, P.; Bresciani, A.; Gennari, N.; Cecchetti, O.; Monteagudo, E.; Orsale, M. V.; Veneziano, M.; Di Marco, A.; Cellucci, A.; Laufer, R.; Altamura, S.; Summa, V.; Harper, S. Discovery of a Selective Series of Inhibitors of Plasmodium falciparum HDACs. *ACS Med. Chem. Lett.* **2016**, *7*, 454−459.

(17) Full details of this study will be reported elsewhere.

(18) Chou, C. J.; Herman, D.; Gottesfeld, J. M. Pimelic diphenylamide 106 is a slow, tight-binding inhibitor of class I histone deacetylases. *J. Biol. Chem.* **2008**, *283*, 35402−35409.

(19) Kinzel, O.; Llauger-Bufi, L.; Pescatore, G.; Rowley, M.; Schultz-Fademrecht, C.; Monteagudo, E.; Fonsi, M.; Gonzalez Paz, O.; Fiore, F.; Steinkühler, C.; Jones, P. Discovery of a potent class I selective ketone histone deacetylase inhibitor with antitumor activity in vivo and optimized pharmacokinetic properties. *J. Med. Chem.* **2009**, *52*, 3453−3456.

(20) Jones, P.; Altamura, S.; Francesco, R. de; Paz, O. G.; Kinzel, O.; Mesiti, G.; Monteagudo, E.; Pescatore, G.; Rowley, M.; Verdirame, M.; Steinkühler, C. A novel series of potent and selective ketone histone deacetylase inhibitors with antitumor activity in vivo. *J. Med. Chem.* **2008**, *51*, 2350−2353.

(21) Rankovic, Z. CNS Physicochemical Property Space Shaped by a Diverse Set of Molecules with Experimentally Determined Exposure in the Mouse Brain. *J. Med. Chem.* **2017**, *60*, 5943−5954.

(22) For preliminary details on the BBB assay see: Elbaum, D.; Beconi, M. G.; Monteagudo, E.; Di Marco, A.; Quinton, M. S.; Lyons, K. A.; Vaino, A.; Harper, S. Fosmetpantotenate (RE-024), a phosphopantothenate replacement therapy for pantothenate kinase-associated neurodegeneration: Mechanism of action and efficacy in nonclinical models. *PLoS One* **2018**, *13*, No. e0192028.

(23) Calculated using ChemAxon software version 15.

(24) Shamovsky, I.; Connolly, S.; David, L.; Ivanova, S.; Nordén, B.; Springthorpe, B.; Urbahns, K. Overcoming undesirable HERG potency of chemokine receptor antagonists using baseline lipophilicity relationships. *J. Med. Chem.* **2008**, *51*, 1162−1178.

(25) Emmett, M. J.; Lim, H.-W.; Jager, J.; Richter, H. J.; Adlanmerini, M.; Peed, L. C.; Briggs, E. R.; Steger, D. J.; Ma, T.; Sims, C. A.; et al. Histone deacetylase 3 prepares brown adipose tissue for acute thermogenic challenge. *Nature* **2017**, *546*, 544−548.